Cell-mediated Transfer of Catalase Nanoparticles from Macrophages to Brain Endothelial and Neural Cells

Matthew J. Haney[1,2], **Yuling Zhao**[1,2], **Shu Li**[1,2], **Sheila M. Higginbotham**[1,2], **Stephanie L. Booth**[1,2], **Huai-Yun Han**[1,2], **Joseph A. Vetro**[1,2], **R. Lee Mosley**[1,3,4], **Alexander V. Kabanov**[1,2,5], **Howard E. Gendelman**[1,2,3,4], and **Elena V. Batrakova**[1,2,*]

[1]Center for Drug Delivery and Nanomedicine, University of Nebraska Medical Center, Omaha, Nebraska, USA

[2]Department of Pharmaceutical Sciences, University of Nebraska Medical Center, Omaha, Nebraska, USA

[3]Center for Neurodegenerative Disorders, University of Nebraska Medical Center, Omaha, Nebraska, USA

[4]Department of Pharmacology and Experimental Neuroscience, University of Nebraska Medical Center, Omaha, Nebraska, USA

[5]Department of Chemical Enzymology, Faculty of Chemistry, M.V.Lomonosov Moscow State University, Moscow, Russia

Abstract

Background—Our laboratories forged the concept of macrophage delivery of protein antioxidants to attenuate neuroinflammation and nigrostriatal degeneration in Parkinson's disease (PD). Notably, the delivery of the redox enzyme, catalase, incorporated into a polyion complex micelle ("nanozyme") by bone marrow-derived macrophages protected the nigrostriatal against 1-methyl-4-phenyl-1,2,3,6-tetrahydropyridine (MPTP) intoxication. Nonetheless, how macrophage delivery of nanozyme increases the efficacy of catalase remains unknown.

Methods—Herein, we examined the transfer of nanozyme from macrophages to brain microvessel endothelial cells, neurons and astrocytes.

Results—Facilitated transport of the nanozyme from macrophages to endothelial and neural target cells occurred through endocytosis-independent mechanisms that involved fusion of cellular membranes; macrophage bridging conduits; and nanozyme lipid coatings. Nanozyme transfer was operative across an artificial blood brain barrier and showed efficient reactive oxygen species decomposition.

Conclusion—This is the first demonstration that drug-loaded macrophages discharge particles to contiguous target cells for potential therapeutic brain enzyme delivery. The pathways for drug delivery shown may be used for the treatment of degenerative disorders of the nervous system.

Keywords

blood-brain barrier; bone marrow-derived macrophages; cell-mediated drug delivery; intercellular communication; Parkinson's disease

*Correspondence: Elena V. Batrakova, Center for Drug Delivery and Nanomedicine, 985830 Nebraska Medical Center, Omaha, NE 68198-5830; Tel: (402) 559-9364; Fax (402) 559-9365, ebatrako@unmc.edu.

INTRODUCTION

Alzheimer's and Parkinson's diseases (AD and PD) are amongst the faster growing disorders in disease prevalence and incidence for the 21st century. The need to develop neuroprotectants and to control neuroinflammation for protection of the brain against injury cannot be overstated [1–3]. To this end, we developed cell based drug delivery systems that uses mononuclear phagocytes (MP; monocytes and macrophages) loaded with an antioxidant enzyme, catalase, to abrogate disease-linked oxidative stress [4, 5]. Block ionomer complexes were used to preclude enzyme degradation with catalase packaged into particles of nanoscale size and termed "nanozymes." We demonstrated that these nanozymes when loaded into bone marrow-derived macrophages (BMM) abrogate inflammation and neurodegeneration in laboratory and rodent models of human PD [4, 5]. Positively-charged block copolymers, polyethyleneimine-poly(ethylene glycol) (PEI-PEG) and poly(L-lysine)-poly(ethylene glycol) proved superior for enzyme delivery and demonstrated limited cytotoxicity with optimal loading, release and enzyme activity preservation inside cells [6].

Nanotoxicology must be a consideration in the development of any inflammatory-response cell based drug delivery system. Although monocyte-macrophages (MDM) are readily attracted to sites of disease pathology by chemokines, the same cells are known to release reactive oxygen species (ROS) and other cytotoxins. Indeed, a range of therapeutic strategies for neurodegenerative disorders are based on attenuating neuroinflammatory responses and macrophage infiltration to sites of tissue injury [7]. Although studies so far have not reported any cytotoxic effects secondary to macrophage-mediated nanoparticle drug delivery translation of such recent inventions to clinical practice have not yet occurred. Encouraging data obtained from rodents demonstrate, on the contrary, that administration of macrophages loaded with catalase nanozyme diminish micro- and astro- gliosis in mouse models of neurodegenerative disorders [5].

The high efficacy achieved is likely linked to brain targeting in the abilities of BMM loaded with nanozyme to cross the blood brain barrier (BBB) and release catalase at the site of disease (particularly, in substantia nigra pars compacta, *SNpc*). Nanozymes are slowly released from BMM in blood with subsequent enzyme delivery to effected brain regions. Moreover, BMM-released catalase in the reticuloendothelial system (liver and spleen) suppress peripheral leukocyte activation decreasing the ingress of inflammatory responses in the brain and increasing protection against 1-methyl-4-phenyl-1,2,3,6-tetrahydropyridine (MPTP)-induced neurodegeneration [5]. Here we report an as yet undisclosed pathway for intercellular transport of nanozyme from BMM to contiguous neural cells including brain microvessel endothelial cells (BMVEC), neurons, and astrocytes. The nanozyme transfer from macrophage to the recipient cells was significantly greater when neural cells were incubated directly with the nanoparticle. Facilitated macrophage-mediated nanozyme transport involved direct nanozyme transfer from BMM to its target cells through partial transient fusion of cellular membranes, formation of macrophage bridging conduits, microtubules, and nanozyme lipid coatings from cell-carriers that increased cell membranotropic properties and permeability. Such biological properties for nanozyme cell transfer can facilitate BBB penetration, affect efficient reactive oxygen species (ROS) decomposition in activated macrophages and increase subsequent neuronal survival. The data taken together support the importance of macrophage-based nanozyme carriage for neurodegenerative diseases, and notably PD.

MATERIALS AND METHODS

Reagents

1,1'-dioctadecyl-3,3,3',3'-tetramethylindodicarbocyanine perchlorate (DID) and 3,3'-dilinoleyl-oxacarbocyanine perchlorate (DIO) were purchased from Invitrogen (Carlsbad, CA, USA). Lipopolysaccharides (LPS), Sephadex G-25, Triton X-100, and trypsin, were purchased from Sigma-Aldrich (St. Louis, MO, USA). Catalase from bovine liver erythrocytes was provided by Calbiochem (San Diego, CA, USA). Methoxypolyethylene glycol epoxy (Me-PEG-epoxy) was purchased from Shearwater Polymer Inc. (Huntsville, AL, USA). Polyethyleneimine-poly(ethylene glycol) (PEI (2K)-PEG (10K)) was synthesized as described [4] by conjugation of PEI and Me-PEG-epoxy. Interferon gamma (IFN-γ) was purchased from Peprotech Inc. (RockyHill, NJ, USA). ^{3}H-labeled catalase was custom-synthesized by PerkinElmer Life (Boston, MA, USA).

Catalase Nanozyme

The polycomplex was produced by mixing catalase and a block copolymer, PEI-PEG, which form nanoparticles with an enzyme-polyion complex core and PEG corona [4, 5]at charge ratio (Z = 1). This was calculated by dividing the amount of aminogroups in the block copolymer protonated at pH 7.4 [8] by the total amount of Gln and Asp in catalase.

Cells

Bone marrow-derived macrophages (BMM) were extracted from femurs of C57Bl/6 male mice 6 – 7 weeks of age [9] and cultured for 10 days in Dulbecco's Modified Eagle's Media (DMEM) (Invitrogen, Carlsbad, CA, USA) supplemented with 1,000 U/mL macrophage colony-stimulating factor (MCSF), a generous gift from Pfizer Pharmaceuticals, Cambridge, MA, USA. Human monocytes were obtained from leukopaks of healthy donors, purified by countercurrent centrifugal elutriation [10] and cultured in DMEM, 1000U/mL MCSF, 10% pooled human serum, 5mL 200mM L-glutamin, 2mL 50 mg/mL gentamicin, and 10ug/mL ciprofloxacin.

To evaluate the macrophage-mediated transfer of nanozyme across the BBB *in vitro*, cell monolayers that exhibit specific characteristics of a mature BBB (*i.e.* tight junctions, drug efflux transporters, and low pinocytic activity [11, 12]) were used. The cell lines employed included mouse immortalized brain microvessel endothelial cells (BMVEC), bovine brain microvessel endothelial cells (BBMEC), and human epithelial colon carcinoma cells (Caco-2). Brain microvessel endothelial cells from mouse, BMVEC, and bovine, BBMEC, sources were used to evaluate species restrictions as they affected nanozyme transfers. In addition, Caco-2 cells were investigated in transport studies based on their structural integrity as compared to brain endothelial cells. The latter are presumed targets for transport of free nanozyme and nanozyme loaded into macrophages.

Mouse BMVEC were isolated from mouse brains of 6–8 week old homozygous male H-2Kb-ts-A58 mice (Immortomouse®, Charles River Labs) with slight modification [13]. Briefly, whole brains were removed, weighed and washed with Mince Buffer (HBSS, amphotericin B [5.0 µg/mL], gentamicin [50 µg/mL], penicillin G [100 U/mL], streptomycin sulfate [100 µg/mL]). The brains ~1 mm sized fragments were incubated in 0.5% collagenase type 1 (Worthington Biochemical Corporation, Lakewood, NJ; 1 mL of collagenase per g of whole brain) for 40 minutes at 37°C, and then centrifuged at 400g for 10 min. The pellet was washed 2X with 20% complete DMEM (DMEM, FBS 20% 1mM L-glutamine, 2 mM Glutamax™, 1 mM sodium pyruvate, 0.1 mM non-essential amino acids, 1X vitamins, 5.0 µg/mL amphotericin B [Fungizone™], 50 µg/mL gentamycin, 100 U/mL penicillin G, 100 µg/mL streptomycin sulfate), filtered with a 70 µm nylon cell strainer (BD

Falcon, Bedford, MA), spun at 400g for 10 minutes at 4°C, and cultured in 20% complete DMEM at 33°C, 5% CO2 in flasks precoated with 1% gelatin. BMVEC were isolated from heterogeneous populations of brain cells by FACS sorting after blocking with mouse BD Fc block (BD Biosciences, San Jose, CA) and double staining for TNF-α-inducible (20 µg murine TNF-α (Peprotech) / mL at 33°C for 4–6 hours), and for V-CAM-1/E-selectin expression [13] using fluorescein rat anti-mouse CD106/VCAM1 (1.5 µg/1×10^6 cells; Clone M/K-2: Southern Biotech, Birmingham, AL) and R-phycoerythrin rat anti-mouse CD62E/E-Selectin/ELAM-1 (1.5 µg/1×10^6 cells; Clone 10E9.6: BD Biosciences, San Jose, CA). Sorted cells were cultured in 6-well plates coated with 0.2% gelatin in DPBS and passaged upon confluence up to passage 20. All procedures were approved by IACUC following appropriate guidelines.

Bovine brain microvessel endothelial cell (BBMEC) were isolated from fresh cow brains by enzymatic digestion and density centrifugation and grown until confluent (typically 12 days) [14]. The BBMEC were maintained in MEM:F12 culture medium supplemented with 10% horse serum, heparin sulfate (100 µg/mL), amphotericin B (2.5 µg/mL), and gentamicin (50 µg/mL). Human colon carcinoma (Caco-2) cell line was obtained from ATCC and cultured in DMEM, containing 10% heat-inactivated FBS, 1% non-essential amino acids, benzylpenicilin (100 U/ml) and streptomycin (10 µg/ml) [15].

Mouse catecholaminergic Cath.A neurons were purchased from American Type Culture Collection (American Type Culture Collection, ATCC, Manassas, VA, USA) and cultured in RPMI-1640 medium supplemented with 8% normal horse serum (NHS), 4% fetal bovine serum (FBS), and 1% penicillin-streptomycin. Cath.A neurons were differentiated by adding 1 mM of N6,2'-O-dibutyryladenosine 3',5'-cyclic monophosphate sodium salt (dbcAMP, St. Louis, MO, USA) [16].

Astrocytes from rat brain frontal cortex tissue (CTX TNA2) were purchased from ATCC and cultured in DMEM medium supplemented with 10% FBS, 4.5 g/L glucose, L-glutamine, 110 mM sodium pyruvate, and 1% penicillin-streptomycin.

Alexa Fluor and Rhodamine Isothiocyanate (RITC) Labeled Catalase

Catalase was labeled with Alexa Fluor 594 or 647 Protein Labeling Kit (Molecular probes, Inc., Eugene, OR, USA), or RITC [4]. Labeled catalase was purified from low molecular weight residuals by gel filtration on a Sephadex G-25 column and lyophilized.

Catalase Nanozyme BMM Loading

BMM grown on T75 flasks ($1–2 \times 10^6$ cells/flask) were pre-incubated with assay buffer (122 mM NaCl, 25 mM NaHCO$_3$, 10 mM glucose, 3 mM KCl, 1.2 mM MgSO$_4$, 0.4 mM K$_2$HPO$_4$, 1.4 mM CaCl$_2$ and 10 mM HEPES), and then the cells were supplemented with the fluorescently-labeled catalase nanozyme (Z =1, 0.5 mg/ml) in assay buffer for one hour at 37°C [4]. After the incubation, the cells were washed three times with ice-cold PBS and used in further experiments. The estimated levels of accumulated nanozyme were 25 µg/1×10^6 cells.

Fluorescence Activated Cell Sorting (FACS)

Amount of fluorescently labeled nanozyme accumulated in target cells was measured by FACS. Typically, monolayers of brain microvessel endothelial cells (BMVEC, or BBMEC), Cath.A neurons, or astrocytes seeded in 6-well plates (1×10^6 cells/well) were allowed to attach over night, and then incubated for various time intervals with BMM (1×10^6 cells/well) loaded with catalase nanozyme or identical concentration of free nanozyme (without BMM). To load BMM with nanozyme, the cell-carriers were incubated with catalase

nanyme (0.5 mg/ml, the highest non-toxic concentration of nanozyme) as previously reported [5]. At these levels, one million BMM re-suspended in 1 ml of the media accumulated 25 µg of nanozyme. The same concentration of free nanozyme was used to compare nanozyme transferred from macrophages to endothelial and neural cells. Following incubation, all cells were collected and the amount of nanozyme accumulated in the receiver cells was assessed by FACS. To distinguish between the cell-carriers and target cells, BMM were labeled with Alexa 678-conjugated Ab to CD 11b prior to the addition. To determine whether cellular adhesion is required for nanozyme transfer, accumulation levels of RITC-labeled nanozyme transferred from BMM to target BBMEC or neurons was assessed in the presence of two adhesion inhibitors, trypsin (0.05%) or locostatin (50 µM). To evaluate effect of energy depletion on nanozyme transfer from BMM, the target cells were pre-incubated in glucose-free buffer with 50 mM 2-Deoxy-glucose (2-DG) and 150 µM NaN_3 for one hour.

Confocal Microscopy

BMVEC and Cath.A neurons grown in the chamber slides [17] at a concenetration of 2×10^5 cells/chamber were co-cultivated with BMM loaded with RITC-labeled nanozyme (1×10^6 cells/chamber) and examined by a confocal fluorescence microscopy (ACAS-570 Meridian Instruments, Okimos, MI, USA) with argon ion laser and corresponding filter set. Digital images were obtained using the CCD camera (Photometrics) and Adobe photoshop software. In some experiments cells nuclear were stained with DAPI (300 µM).

To confirm actual transport of catalase from macrophages to target cells, BMM were loaded with non-labeled human catalase nanozyme, and added to BMVEC as described above. Following incubation, the cells were fixed with 4% paraformaldehyde (PFA) for 15 min, permeabilized with 0.4% Triton for 4 min, and stained with primary mouse Ab to human catalase (Abcam #ab16772-100, Boston, MA, USA), and Alexa 567-conjugated secondary goat anti mouse Ab (1:200 Dilution, Invitrogen, Carlsbad, CA, USA). Non-specific interactions were blocked with 3% BSA for 30 min prior the staining with Ab. To distinguish between the cell-carriers and receiver cells, BMM were labeled with Alexa 488-conjugated Ab to CD 11b prior to the addition to receiver cells.

[3]H-labeled Nanozyme Permeability Studies

Confluent primary brain microvessel endothelial and epithelial cell monolayers retain morphological and biochemical BBB characteristics [11]. The evaluation of monocyte [18] and nanoparticle trafficking [19–21] across an *in vitro* BBB was investigated previously in our laboratories. Herein, BBMEC or Caco-2 monolayers cultured in 12-well transwell inserts with trans-epithelial electrical resistance (TEER) above 190 $\Omega \cdot cm^2$ or 220 $\Omega \cdot cm^2$ (for BBMEC and Caco-2, respectively) were used for transport studies. BMM loaded with ^{3}H-labeled nanozyme [4] were added in the upper chamber of BBMEC or Caco-2 monolayers at concentration of 1×10^6 cells/well. TNF-α (150 ng/ml, R&D Systems, Minneapolis, MN, USA) was placed into the lower chamber and used as a chemoattractant [18]. Free ^{3}H-labeled nanozyme at identical concentration (25 µg/ml, 2.2 µCi/ml) was used with control monolayers. Appearance of nanozyme in the receiver chamber was monitored by radioactive count at various time intervals (0 – 360 min). All experiments were performed in quadruplicate.

Antioxidant Activity Measurements

The ability of BMM loaded catalase nanozyme to scavenge hydrogen peroxide produced by activated human blood monocytes was tested by Amplex Red. A linear dependence of the catalytic activities on the enzyme concentrations was observed in the range of 0–1.0 mg/ml [6]. Human monocytes seeded in 96-well plates at a concentration of 0.1×10^6 cells/well

were stimulated with LPS, 20 ng/ml and IFN-γ, 2 µg/ml for 24 hours to induce ROS production. Following incubation, the cells were supplemented with various concentrations (5–50 µg/ml) of nanozyme loaded into BMM or nanozyme alone at the same concentrations for another hour. Then cells were supplemented with Amplex Red Dye stock solution (10 U/mL HRP, 10 mM Ampex Red) for 30 minute, and ROS content was measured by fluorescence at λ_{ex}=563 nm, λ_{em}=587 nm according to the manufacturer's specifications. Data represents ± SEM (n=4).

Statistical Analysis

For the all experiments, data are presented as the mean ± SEM. Tests for significant differences between the groups were done using a one-way ANOVA with multiple comparisons (Fisher's pairwise comparisons) using GraphPad Prism 5.0 (GraphPad software, San Diego, CA, USA). A minimum p value of 0.05 was estimated as the significance level for all tests.

RESULTS

Macrophage-facilitated Transport of Nanozyme to Target Cells

The transport of RITC-labeled catalase from carrier BMM to BMVEC, neurons, and astrocytes, was examined. Given their involvement in the pathology of neurodegeneration, these target cells represent potential sites for therapy. Target cells were incubated with nanozyme alone or BMM loaded nanozymes at equivalent enzyme concentrations (25 µg/mL) for 0.5 – 4.0 hours, and nanozyme concentrations in target cells were assessed by FACS (Figure 1). Representative FACS plots are in supplementary material (Figure S1A). Nanozyme transfer from BMM to all target cells (black bars) was greater than free nanozyme (white bars), especially at later time points (Figure 1). Interestingly, mouse BMM transferred nanozymes both syngeneically to mouse BMVEC (Figure 1A) and xenogeneically to bovine BMVEC (Figure S1B), indicating no species restrictions.

A time course of RITC-labeled nanozyme transfer from BMM to BMVEC (Figure 2A, Media S1) and Cath.A neurons (Figure 2B) was evaluated by confocal microscopy. Nanozymes localized in BMVEC at the sites of contact with donor BMM (Figure 2A, B shown by arrows). In contrast, free nanozymes diffused over the entire BMVEC monolayer (Figure S2). For BMM-Cath.A, initiation at axonal sites was observed with BMM contact that was followed by retrograde transfer of nanozymes into the neuronal cell body (Figure 2B, shown by arrows). Interestingly, no prolonged attachment of BMM to the target cells was required for nanozyme transfer (Media S1).

To ensure the fluorescent staining reflected the intracellular localization of nanozyme and not free fluorescent dye, inactive enzyme components, or cell surface associated nanozyme, mouse BMM loaded with non-labeled human catalase nanozyme were incubated with mouse BMVEC for two hours, fixed, permeabilized, and stained with primary Ab to human catalase (Figure S3). Catalase accumulated in macrophages and in the BMVEC (shown by arrows). No catalase was observed with non-permeabilized monolayers of nanozyme-loaded BMM incubated with BMVEC, indicating that nanozyme was transferred inside the cells and not onto the cell surface (data not shown).

Cell-Cell Contact and Adhesion for Nanozyme Transfers

Relationships between BMM and BMVEC cells were evaluated through accumulation of RITC-labeled nanozyme from BMM with and without direct cell-cell contact (Figure 3A). The substantial nanozyme transfer was recorded even without direct contact (Figure 3B),

although, it was significantly greater when the contact between the donor and target cells was allowed, indicating its importance for the efficient nanozyme transfer.

To determine whether cellular adhesion is required for nanozyme transfer, accumulation levels of RITC-labeled nanozyme transferred from BMM to target BBMEC or neurons were assessed in the presence or of absence two adhesion inhibitors, trypsin or locostatin. Nanozyme transfers were not affected by the adhesion inhibitors (Table 1). Overall, rapid movement of BMM and nanozyme administered to BMVEC (Media S1) support the idea of transient cell-cell interactions during cell cultivation for up to two hours.

Transport of Nanozyme through Microtubules

It was demonstrated previously that macrophages infected with HIV-1 virus particles can transfer them into uninfected cells through bridging conduits (BCs), filopodia and elongated lamellipodia [22, 23]. These cytoskeleton components are essential for cytoplasmic exchanges as well as cell signaling and migration. To this end, we examined involvement of BCs in nanozyme transfer from BMM to target cells at > two hours (Figure 4). BMM loaded with RITC-labeled nanozyme (red) formed multiple filopodia filled with nanozyme (Figure 4 A, B, shown by white arrows) that were stretched to the DIO-labeled BMVEC (green). Human macrophages (green) formed elongated lamellipodia filled with nanozyme (red) over the course of 18 hours (Figure S4). This suggests that the BCs connected cells and as such facilitated nanozyme transfer. Partial co-localization of actin microfilaments and nanozyme indicated involvement of microtubules network in nanozyme transfer (Figure 4 C–E). Interestingly, two types of host cells were detected: i) transporting macrophages with strong actin and nanozyme co-localization (Figure 4 C–E, shown by white arrows), and ii) resting cells with very little co-localization (Figure 4 C and F, shown by green arrows). We posit that membrane contacts of cell-carriers with the target cells may activate BMM and initiate nanozyme transport by microtubules.

Transfer of Nanozyme Laden Lipids from BMM

We hypothesized that nanozymes are transferred to target cells with BMM components including proteins or lipids. Thus, we assessed the possible involvement of lipid compartments in cell-cell transfers of nanozymes by FACS and confocal microscopy (Figures 5–7). Loaded with nanozyme and stained with DIO lipophilic dye BMM (Figure 5 A) were incubated with stained with DID Cath.A neurons (Figure 5 B). Substantial amount of co-cultured cells carried both dyes after two hours of incubation (Figure 5 C and D). Notably, lipid compartment transfer occurred from BMM to neurons but at an even greater extent from neurons to BMM (Figure 5 D). Similar lipid exchange was observed for BMM-BMVEC cell pair by confocal microscopy (Figure 6) showing vesicle-like inclusions with BMM lipids (red) in BMVEC (Figure 6 A, B, shown by arrows), and BMVEC lipids (green) in BMM (Figure 6 C, D). Corroborative evidence of concurrent transfer of nanozyme and lipid compartments was obtained with BMM-neurons pair. Accumulation and co-localization of BMM lipids (green) with nanozyme (red) in non-stained Cath.A neurons was manifested by yellow staining (Figure 7, shown by arrows). Overall, the data suggests that nanozyme was wrapped into lipids from BMM, which increased membranotropic properties and facilitate nanoparticle transfer amongst the cells.

To test this, accumulation levels of freshly prepared or released from BMM nanozyme were compared in Cath.A neurons (Figure 8 A). Transfer of nanozyme released from BMM was significantly greater than freshly prepared nanoparticles (Figure 8 B) confirming its facilitated transport from BMM to co-cultured target cells.

Effect of Energy Depletion on Nanozyme Cell Transfer

Proteins and nanoparticles, such as nanozymes, accumulate in cells predominantly by endocytosis, an ATP-dependent process. To determine whether this mechanism is involved in the BMM-mediated nanozyme transfer, accumulation levels of free or loaded in BMM nanozyme in target cells (BMVEC, BBMEC, and Cath.A neurons) was assessed under homeostatic conditions or at energy-depletion state. Accumulation of free nanozyme was significantly decreased by ATP depletion in the target cells (Table 2). In contrast, nanozyme transport from BMM was unaffected suggesting that this process is endocytosis-independent. Both bovine and mouse BMVEC showed identical mechanism, re-affirming that nanozyme transfer is not species specific.

BMM-mediated Transfer of Nanozyme in an Artificial BBB Model

Given the obtained data, we hypothesized that nanozyme facilitated transfer to BMVEC from BMM might result in improved BBB penetration compared to free nanozyme. BBMEC [11] and Caco-2 [12] monolayers that exhibit BBB functional properties, were used to test this hypothesis. Transport of nanozyme loaded into BMM was substantially greater than free nanozyme in both systems (Figure 9 A, B). The advantage of cell-mediated transfer was even more evident in Caco-2 in vitro model, probably, due to the fact that the epithelial cell monolayers are less leaky than BBMEC (see **Materials and Methods** section).

Antioxidant Activity of Nanozymes

Given facilitated nanozyme transfer from BMM, it may eliminate ROS more efficiently than free nanozyme. Human monocytes stimulated with lipopolysacharide (LPS) and interferon gamma (IFN-γ) were used to test this hypothesis. This reflects, in part, the inflammatory environment that blood borne brain macrophages and microglia find themselves in during progressive neurodegenerative diseases such as PD. Following activation, the cells were supplemented with various concentrations of free nanozyme or nanozyme loaded into BMM (Figure 9 C). Quiescent monocytes (unactivated, first bar) or LPS/IFN-γ activated cells without subsequent treatment with nanozyme (second bar) were used as a control. Nanozyme loaded in BMM has greater antioxidant activity than the identical concentrations of free enzyme (Figure 9 C), probably, due to the facilitated transport of nanozyme from macrophages to the adjacent target cells.

DISCUSSION

The ability to communicate between cells is crucial for the survival of large multicellular organisms as it allows coordinating their functional activities at the organ level. Divergent types of cells show exchange of organelles and endogenous molecules between one other. The most known example is a transfer of neurotransmitters in neurons [24]. Cell-to-cell exchange of viral particles was reported in plants [25] and eukaryotic cells [26, 27]. In particular, it was demonstrated that HIV-1 spreads from uninfected to infected cells through bridging conduits mediated by endocytic trafficking [22, 23]. Importantly, this transport occurs in non-degraded cargoes caring functionally active viral constituents capable of proviral integration and expression in the target uninfected cells. This adverse mechanism of viral dissemination that shelters HIV-1 providing systemic infection and disease progression may play positive role in case of cell-mediated drug delivery, where preservation of enzymatic activity of the drug (herein catalase) in the cell-carriers is crucial.

Macrophages were already shown to serve as vehicles for nanoformulated antiretroviral drug delivery [28–30]. Additional works indicated that they may also be harnessed for therapeutic use for a range of CNS disorders, such as HIV-associated neurocognitive disorders, cerebrovascular diseases, and neurodegenerative disorders, AD and PD [9, 31–33]. In this

respect to improve drug transport across the BBB, we developed a new drug delivery system using specific cells-carriers that can incorporate nanocontainers loaded with drugs and act as perfect Trojan horses migrating across the BBB to deliver drugs to sites. Indeed, MPs loaded with catalase nanozyme can attenuate neuroinflammation and neurodegeneration in models of PD [4, 5]. The present work developed new insights into how the cell-carriers can yield superior clinical results from nanoparticles administered alone. This involves facilitated transfer of drug-loaded nanoparticles from MPs to target cells that are intimately involved in the development of neurodegenerative disorder itself such as BMVEC, neurons, and astrocytes.

We report here for the first time to the best of our knowledge that macrophages, loaded with nanozyme, promote its accumulation in the target cells indicated above. Interestingly, increased transfer was observed for the same species donor-receiver cell pair (C57Bl/6 mouse), as well as for different hosts cell pairs (mouse-rat, mouse-bovine, and mouse-human). Staining with fluorescently-labeled Ab to catalase confirmed the intercellular transfer of nanozyme and not free fluorescent dye, inactive enzyme components or cell surface associated nanozyme. The dynamic of nanozyme cell-to-cell transfer revealed initial localized distribution of nanozyme in the receiver cells at the sites of their contact with the donor BMM, in contrast, free nanozyme that diffused over entire cell monolayer. Retrograde transfer of nanozymes from BMM initiated at the axon site was observed in the neuronal cell body.

Cell-to-cell contact plays an important role in this transfer, although, no prolonged attachment of BMM to the target cells was required for nanozyme transfer. Thus, macrophages placed on the top of BMVEC monolayers transferred significantly greater amount of nanozyme compared to the same amount of cell-carriers localized in 2–4 mm above the target cell. Nevertheless, adhesion of macrophages onto the receiver cells is not required for the successful transfer of nanozyme at least for the first two hours of incubation. In particular, target cells (BMVEC or neurons) that were pre-incubated with adhesion inhibitors, trypsin or locostatin, accumulated the same amount of nanozyme as the cells in the absence of the inhibitors. It is likely that that partial transient fusion of the cell membranes is involved in this transfer.

Over longer time periods (2–18 hours), the loaded macrophages developed filopodia and lamellipodia filled with nanozyme that was involved in cell-to-cell drug transfer. Interestingly, confocal images revealed two types of cell-carriers: i) "transporting" macrophages with strong co-localization of nanozyme and actin microfilaments, and ii) "resting" macrophages where nanozyme is stored in intracellular compartments distinct from BCs. We speculate that macrophages coming in contact with the target cells become activated and initiate nanozyme transfer using actin microphilaments as tracks.

Nanozyme was transferred along with lipids from cell-carriers. A strong co-localization of fluorescently-labeled nanozyme and lipids of the BMM was demonstrated in BMVEC and neuron targets. In fact, we do not exclude that nanozyme might be transported along with whole lipid and protein-containing compartments from macrophages into target cells. Such "coating" should increase membranotropic properties and facilitate intracellular transport of nanozyme. To separate this process from the nanozyme transfer through the transient membrane fusion, the accumulation levels of nanozyme released from BMM was compared with the fresh prepared nanozyme. Accumulation of nanozyme released from BMM was significantly greater than fresh prepared nanozyme. It signifies that the observed facilitated nanozyme transfer may be, in part, due to the nanozyme lipid coating and subsequent biding with the lipid membranes of the target cells. We hypothesized that such coating may occur when nanozyme is released from BMM in exosomes. The similar phenomenon was reported

for virus particles [34]. In fact, nanozyme transfered through transient membranes fusion and BCs formation may also be incorporated in such compartments.

All above mentioned mechanisms may completely change the mechanism of nanozyme entry in the receiver cells. Indeed, intercellular nanozyme transfer was not affected by energy depletion in the target cells, suggesting that neither the cell-to-cell transfer by transient membrane fusion or developing filopodia and lamellipodia, nor the transfer of lipid-coating of nanoparticles involves endocytosis.

The observed phenomena may have significant therapeutic outcomes. Specifically, nanozyme-loaded BMM efficiently transfer nanoparticles into BMVEC may facilitate their delivery to the brain parenchyma enhancing BBB permeability and CNS drug transport. Furthermore, drug-loaded cell-carriers reaching the inflamed brain areas may infuse/unload active nanozyme into neurons, astrocytes or microglial cells with efficient ROS decomposition and subsequent reduction of inflammation. Indeed, enhanced transport of nanozyme from cell carriers compared to free nanozyme across BBB in vitro was demonstrated. Nanozyme facilitated transfer resulted in efficient ROS decomposition in activated human monocytes that served as a model of microglial activation.

Previously, we suggested three different mechanisms that may singly or collectively be responsible for improved therapeutic effects of nanozyme loaded into macrophages in mouse PD model (Figure 10) [5]. *First*, BMM loaded with catalase might reach CNS inflammation site and deliver catalase, *i.e.* accomplish targeting delivery of catalase to SNpc. *Second*, nanozyme-loaded BMM might work as a depot for the sustained release of nanoformulated catalase *in vivo*, when the enzyme enters the brain independently of cell-carriers. In fact, we demonstrated that some portion of loaded macrophages migrates from the blood away into the tissue and the tissue-associated BMM slowly unload nanozyme and supply the blood plasma with sustained levels of catalase. *Third*, catalase released from cell-carriers in the liver or spleen (the most enriched organs after transfer of nanozyme-loaded BMM) and produced suppression of peripheral leukocyte activation resulting in significant protection of nigrostratial neurons against MPTP-induced neurodegeneration. The facilitated transfer of nanozyme from the cell-carriers into BMVEC, neurons, and astrocytes, reported here, is an additional *fourth* mechanism. While multiple mechanisms may play roles in neuroprotective effects of nanozymes, cell to cell transfer may be the mechanism that coordinates other mechanisms to strengthen the final therapeutic effect.

CONCLUSIONS

The numbers of cell-carriers that can reach the disease site is crucial in the case of CNS disorders, when drug needs to be delivered cross the BBB to mediate therapeutic effect. In fact, many neurological diseases, such as Alzheimer's and Parkinson's diseases, Prion disease, meningitis, encephalitis and AIDS related dementia, have in common an inflammatory component [35] characterized by extensive immunocyte recruitment to the brain. Based on the cells' presence within the central nervous system during disease, they can reach the brain after peripheral loading with nanoparticles. Nevertheless, nanozyme facilitated transfer from BMM to neural cells, in particular, BMVEC, suggests that drug transport can be accomplished without actual crossing the BBB but through the promoted transport of nanozyme from BMM. This involved fusion of cellular membranes; macrophage bridging conduits; and nanozyme lipid coatings. Such cell-to-cell activites may also improve efficiency of reactive oxygen species (ROS) decomposition by catalase nanozyme in neurons and astrocytes.

EXECUTIVE SUMMARY

- This study, to the best of our knowledge, is the first demonstration of nanoparticular catalase facilitated transport from macrophages into three types of target cells: brain microvessel endothelial cells, neurons, and astrocytes, was demonstrated.

- Cell-to-cell contact between macrophages and receiver cells increases nanozyme transfer, although no adhesion is required.

- Nanozyme transfer occurs through partial transient fusion of donor and receiver cells at shorter time points, or through formation of filopodia and lamellipodia after longer exposure times.

- Nanoparticles are transferred along with lipids from host cells that increased their membranotropic properties and facilitated transport into the target cells.

- Facilitated transport of nanozymes from BMM into target cells occurs through an endocytosis-independent pathway.

- Facilitated transport of nanozyme results in improved penetration across the BBB and ROS dismutation *in vitro*.

Supplementary Material

Refer to Web version on PubMed Central for supplementary material.

Acknowledgments

REFERENCES

1. Brinton, Rd. A women's health issue: Alzheimer's disease and strategies for maintaining cognitive health. Int J Fertil Womens Med. 1999; 44(4):174–185. [PubMed: 10499738]

2. Gozes I. Neuroprotective peptide drug delivery and development: Potential new therapeutics. Trends Neurosci. 2001; 24(12):700–705. [PubMed: 11718874]

3. Kroll, Ra; Neuwelt, Ea. Outwitting the blood-brain barrier for therapeutic purposes: Osmotic opening and other means. Neurosurgery. 1998; 42(5):1083–1099. discussion 1099–1100. [PubMed: 9588554]

4. Batrakova, Ev; Li, S.; Reynolds, Ad, et al. A macrophage-nanozyme delivery system for parkinson's disease. Bioconjug Chem. 2007; 18(5):1498–1506. [PubMed: 17760417]

5. Brynskikh, Am; Zhao, Y.; Mosley, Rl, et al. Macrophage delivery of therapeutic nanozymes in a murine model of parkinson's disease. Nanomedicine (Lond). 2010; 5(3):379–396. [PubMed: 20394532]

6. Zhao Y, Haney M, Klyachko N, et al. Polyelectrolyte complex optimization for macrophage delivery of redox enzyme nanoparticles. Nanomedicine. 2010 in press.

7. Hendriks, Jj; Teunissen, Ce; De Vries, He; Dijkstra, Cd. Macrophages and neurodegeneration. Brain Res Brain Res Rev. 2005; 48(2):185–195. [PubMed: 15850657]

8. Vinogradov S, Bronich T, Kabanov A. Self-assembly of polyamine-poly(ethylene glycol) copolymers with phosphorothioate oligonucleotides. Bioconjugate Chemistry. 1998; 9(6):805–812. [PubMed: 9815175]

9. Dou H, Destache Cj, Morehead Jr, et al. Development of a macrophage-based nanoparticle platform for antiretroviral drug delivery. Blood. 2006; 108(8):2827–2835. [PubMed: 16809617]

10. Srtevenson, Hc; Fauci, As. Purification of human monocytes by counter-current centrifugation elutriation. New York: Marcel Decker Press; 1981.

11. Weidenfeller C, Schrot S, Zozulya A, Galla Hj. Murine brain capillary endothelial cells exhibit improved barrier properties under the influence of hydrocortisone. Brain Res. 2005; 1053(1–2): 162–174. [PubMed: 16040011]

12. Faassen F, Vogel G, Spanings H, Vromans H. Caco-2 permeability, p-glycoprotein transport ratios and brain penetration of heterocyclic drugs. Int J Pharm. 2003; 263(1–2):113–122. [PubMed: 12954186]

13. Langley, Rr; Ramirez, Km; Tsan, Rz; Van Arsdall, M.; Nilsson, Mb; Fidler, Ij. Tissue-specific microvascular endothelial cell lines from h-2k(b)-tsa58 mice for studies of angiogenesis and metastasis. Cancer Res. 2003; 63(11):2971–2976. [PubMed: 12782605]

14. Batrakova E, Han H, Miller D, Kabanov A. Effects of pluronic p85 unimers and micelles on drug permeability in polarized bbmec and caco-2 cells. Pharm Res. 1998; 15(10):1525–1532. [PubMed: 9794493]

15. Fogh J, Fogh Jm, Orfeo T. One hundred and twenty-seven cultured human tumor cell lines producing tumors in nude mice. J Natl Cancer Inst. 1977; 59(1):221–226. [PubMed: 327080]

16. Rosenbaugh, Eg; Roat, Jw; Gao, L., et al. The attenuation of central angiotensin ii-dependent pressor response and intra-neuronal signaling by intracarotid injection of nanoformulated copper/ zinc superoxide dismutase. Biomaterials. 2010; 31(19):5218–5226. [PubMed: 20378166]

17. Batrakova, Ev; Vinogradov, Sv; Robinson, Sm; Niehoff, Ml; Banks, Wa; Kabanov, Av. Polypeptide point modifications with fatty acid and amphiphilic block copolymers for enhanced brain delivery. Bioconjug Chem. 2005; 16(4):793–802. [PubMed: 16029020]

18. Zelivyanskaya, Ml; Nelson, Ja; Poluektova, L., et al. Tracking superparamagnetic iron oxide labeled monocytes in brain by high-field magnetic resonance imaging. J Neurosci Res. 2003; 73(3):284–295. [PubMed: 12868062]

19. Batrakova E, Li S, Alakhov V, Miller D, Kabanov A. Optimal structure requirements for pluronic block copolymers in modifying p-glycoprotein drug efflux transporter activity in bovine brain microvessel endothelial cells. J Pharmacol Exp Ther. 2003; 304(2):845–854. [PubMed: 12538842]

20. Batrakova E, Li S, Miller D, Kabanov A. Pluronic p85 increases permeability of a broad spectrum of drugs in polarized bbmec and caco-2 cell monolayers. Pharm Res. 1999; 16(9):1366–1372. [PubMed: 10496651]

21. Batrakova E, Miller D, Li S, Alakhov V, Kabanov A, Elmquist W. Pluronic p85 enhances the delivery of digoxin to the brain: In vitro and in vivo studies. J Pharmacol Exp Ther. 2001; 296(2): 551–557. [PubMed: 11160643]

22. Kadiu I, Ricardo-Dukelow M, Ciborowski P, Gendelman He. Cytoskeletal protein transformation in hiv-1-infected macrophage giant cells. J Immunol. 2007; 178(10):6404–6415. [PubMed: 17475870]

23. Kadiu I, Gendelman He. Macrophage endocytic trafficking networks facilitate hiv-1 intercellular transport through tunneling nanotubes: A novel pathway for viral dissemination. The Journal of Immunology. 2010 in revision.

24. Krishnamurthy H, Piscitelli Cl, Gouaux E. Unlocking the molecular secrets of sodium-coupled transporters. Nature. 2009; 459(7245):347–355. [PubMed: 19458710]

25. Boyko V, Ferralli J, Ashby J, Schellenbaum P, Heinlein M. Function of microtubules in intercellular transport of plant virus rna. Nat Cell Biol. 2000; 2(11):826–832. [PubMed: 11056538]

26. Sherer, Nm; Lehmann, Mj; Jimenez-Soto, Lf; Horensavitz, C.; Pypaert, M.; Mothes, W. Retroviruses can establish filopodial bridges for efficient cell-to-cell transmission. Nat Cell Biol. 2007; 9(3):310–315. [PubMed: 17293854]

27. Chinnery, Hr; Pearlman, E.; Mcmenamin, Pg. Cutting edge: Membrane nanotubes in vivo: A feature of mhc class ii+ cells in the mouse cornea. J Immunol. 2008; 180(9):5779–5783. [PubMed: 18424694]

28. Nowacek, As; Miller, Rl; Mcmillan, J., et al. Nanoart synthesis, characterization, uptake, release and toxicology for human monocyte-macrophage drug delivery. Nanomed. 2009; 4(8):903–917.

29. Bressani, Rf; Nowacek, As; Singh, S., et al. Pharmacotoxicology for monocyte-macrophage nanoformulated antiretroviral drug carriage. The Journal of Immunology. 2010 in revision.

30. Nowacek, As; Mcmillan, J.; Miller, R.; Anderson, A.; Rabinow, B.; Gendelman, He. Nanoformulated antiretroviral drug combinations extend drug release and antiretroviral responses in hiv-1-infected macrophages: Implications for neuroaids therapeutics. J Neuroimmune Pharmacol. 2010

31. Jain S, Mishra V, Singh P, Dubey Pk, Saraf Dk, Vyas Sp. Rgd-anchored magnetic liposomes for monocytes/neutrophils-mediated brain targeting. Int J Pharm. 2003; 261(1–2):43–55. [PubMed: 12878394]

32. Dou H, Grotepas Cb, Mcmillan Jm, et al. Macrophage delivery of nanoformulated antiretroviral drug to the brain in a murine model of neuroaids. J Immunol. 2009; 183(1):661–669. [PubMed: 19535632]

33. Biju K, Zhou Q, Li G, et al. Macrophage-mediated gdnf delivery protects against dopaminergic neurodegeneration: A therapeutic strategy for parkinson's disease. Mol Ther. 2010; 18(8):1536–1544. [PubMed: 20531393]

34. Thery C, Ostrowski M, Segura E. Membrane vesicles as conveyors of immune responses. Nat Rev Immunol. 2009; 9(8):581–593. [PubMed: 19498381]

35. Perry, Vh; Bell, Md; Brown, Hc; Matyszak, Mk. Inflammation in the nervous system. Curr Opin Neurobiol. 1995; 5(5):636–641. [PubMed: 8580715]
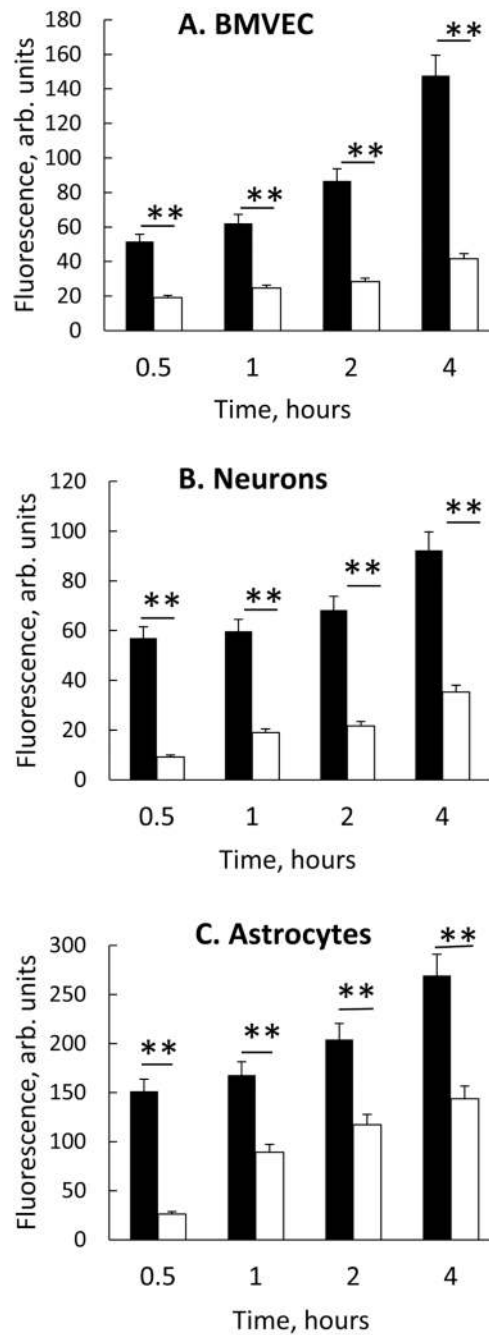
Figure 1. Intercellular transport of nanozyme from BMM to endothelial and neural cells
RITC-labeled nanozyme were loaded to BMM (black bars) or nanozyme were administered alone (white bars) to **A**, murine BMVEC; **B**, CATH.a transformed neurons; or **C**, rat astrocytes for 0.5 to 4 hours. Following incubation, BMM were stained with CD11b Ab (Alexa 488) and the amount of nanozyme that was accumulated in CD11b-negative recipient cells (endothelial cells, neurons or astrocytes) assessed by FACS as mean RITC fluorescence ± SEM (n=4). Nanozyme transfers from BMM to each of the recipient target cells were greater in BMM laden nanozyme co-cultures (black bars) than with free nanozyme (white bars). Significance of BMM nanozyme *vs*. free nanozyme at each time point is shown by asterisk (***p<0.005*).
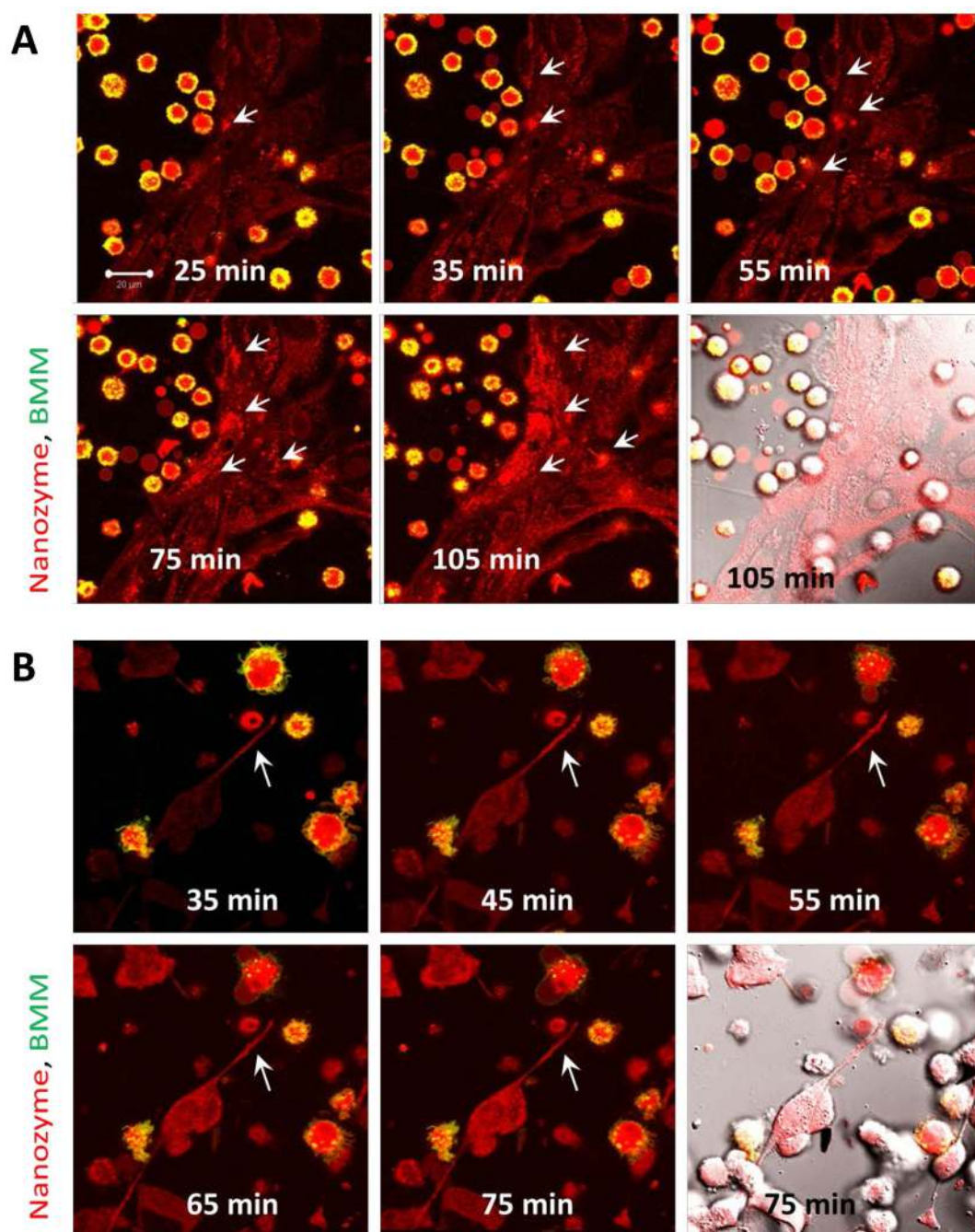
Figure 2. Kinetic transport of nanozymes from BMM to endothelial cells and neurons
Confocal images of murine BMVEC (**A**) or Cath.A neurons (**B**) incubated with BMM loaded with RITC-labeled catalase nanozyme (red). BMM were labeled with Alexa 678-conjugated Ab to CD 11b (green). Co-localization of nanozyme (red) and BMM CD 11b staining (green) was manifested in yellow. The last time point fluorescence image of each set is shown with DIC. Nanozymes were transferred from BMM to BMVEC (**A**) or from BMM to neurons (**B**) at the sites of cell contact with donor cells (shown by arrows). The initiation at the axon sites was observed upon contact with BMM followed by retrograde transfer of nanozymes into the neuronal cell body (**B**). Bar = 20 µm.

A
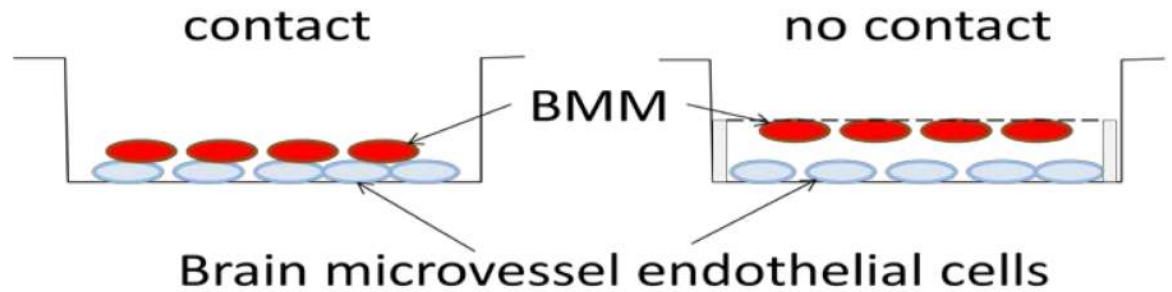
B
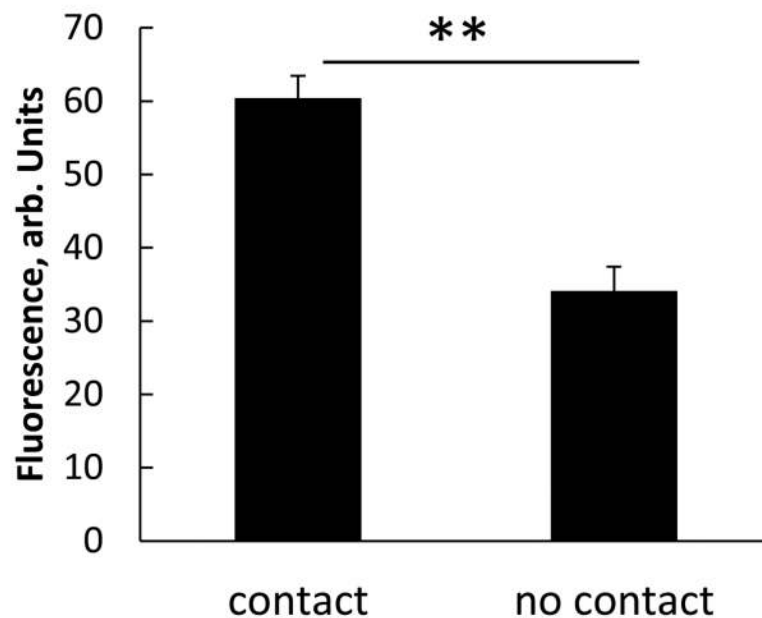
Figure 3. Cell-cell contact facilitate nanozyme transfer from BMM to BMVEC
BMVEC were grown on the bottom of the plate. BMM stained with DID (green) were loaded with RITC-labeled nanozyme (red) and placed: i) on top of BMVEC (contact), or ii) ~two mm above the BMVEC (no contact). In case of "no contact", BMM were attached to a semi-permeable membrane and located on the down side of the membrane. Following a two-hour incubation, the cells were collected and the amount of nanozyme accumulated in the recipient cells assessed by FACS. **A**, experimental scheme; B, average RFU ± SEM (n=3) demonstrating significantly greater nanozyme levels when BMM were in contact with recipient cells and demonstrating the importance of cell-cell communications for nanozyme transfer. Statistical significance was calculated between cell-cell contact *vs.* no cell contact (***p<0.005*).
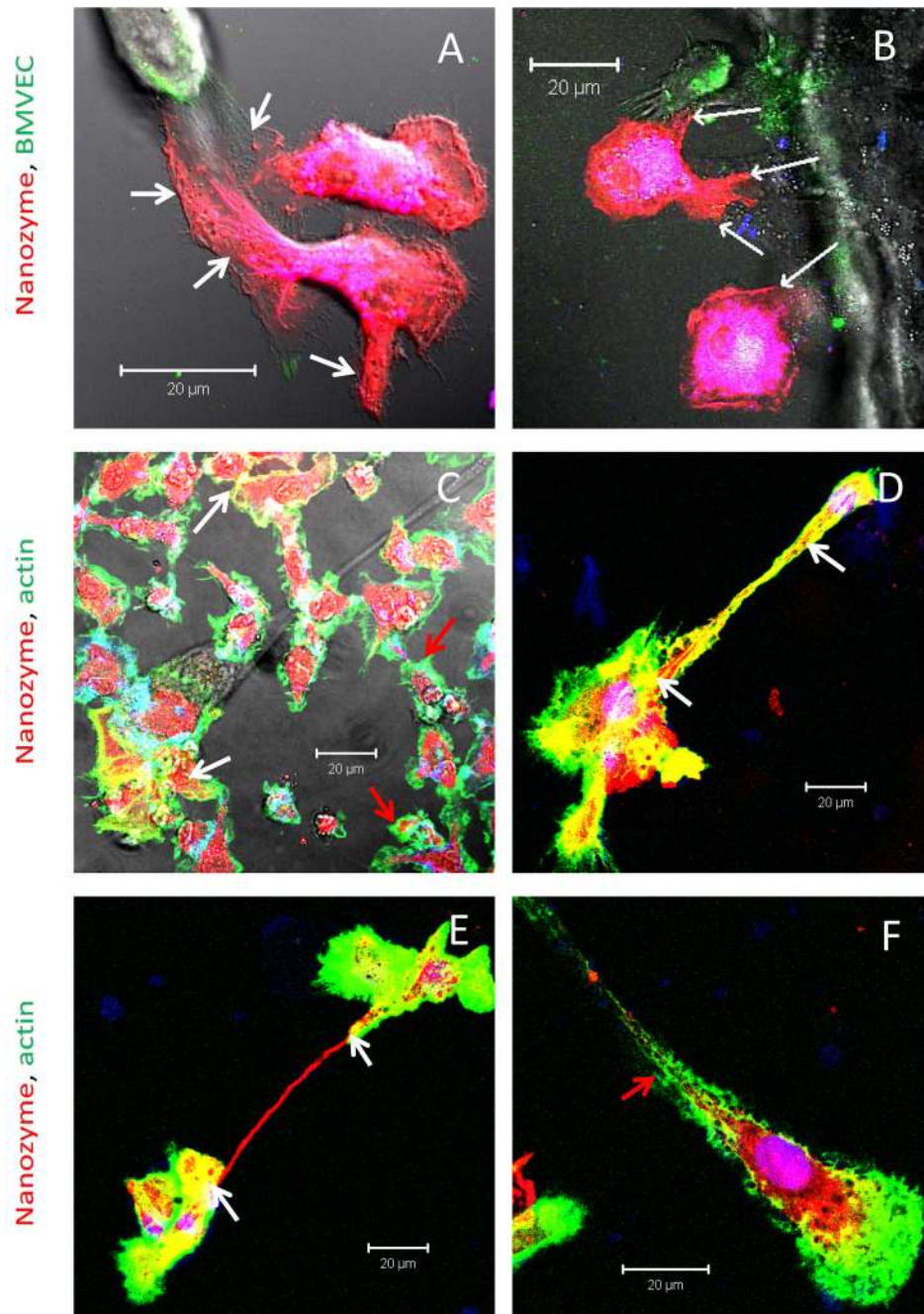
Figure 4. Transfer of nanozyme from BMM to BMVEC is facilitated by BCs
BMM were loaded for 2 hrs with RITC-labeled nanozyme (red), and then co-cultured with DIO-labeled (**A, B**, green) or non-labeled BMVEC (**C–F**) for 18 hours. **C–F**, After incubations cells were fixed, permeabilized and stained with Alexa488-labeled phalloidin to visualize actin filaments (green). Cell nuclei were stained with DAPI. BMM contained multiple filopodia filled with nanozymes (**A, B** white arrows) supporting their involvement in nanoparticles transfer. Actin microfilaments staining (**C–F**) revealed macrophages in two different stages: i) transporting macrophages with actin and nanozyme co-localization (Figure 4 C–E, shown by white arrows); and ii) resting macrophages with limited co-localizations (Figure 4 C and F, shown by red arrows). Bar represents 20 µm.
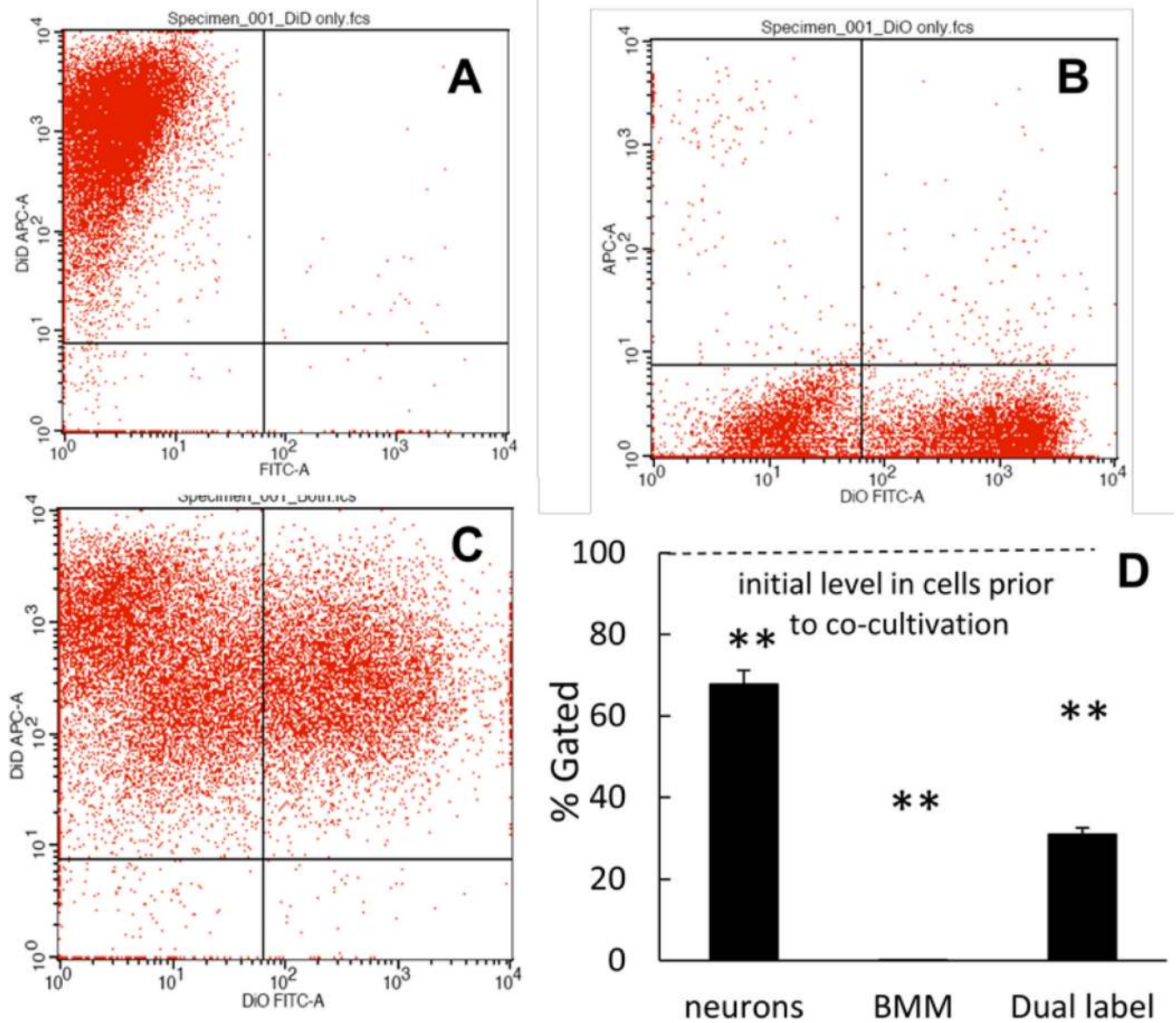
Figure 5. Intercellular exchange of BMM and neuronal lipid compartments
BMM loaded with nanozyme were stained with Alexa 678-conjugated Ab to CD 11b, then incubated with Cath.A neurons stained with DID lipophilic dye. These were performed at 37°C for two hours. Following incubation, percentage of cells which accumulated both dyes were assessed by FACS: **A**, Cath.A neurons stained with DID; **B**, BMM loaded with nanozyme and stained with Alexa 678; **C**, Incubation of Cath.A neurons and BMM; **D**, Quantification of label exchange is shown. Results from N=4 wells (± SEM) demonstrate that Cath.A neurons and BMM (at greater extent) exchange membrane dyes. Statistical significance is shown by asterisk: *p<0.005* (**) compared to what was observed before incubation.
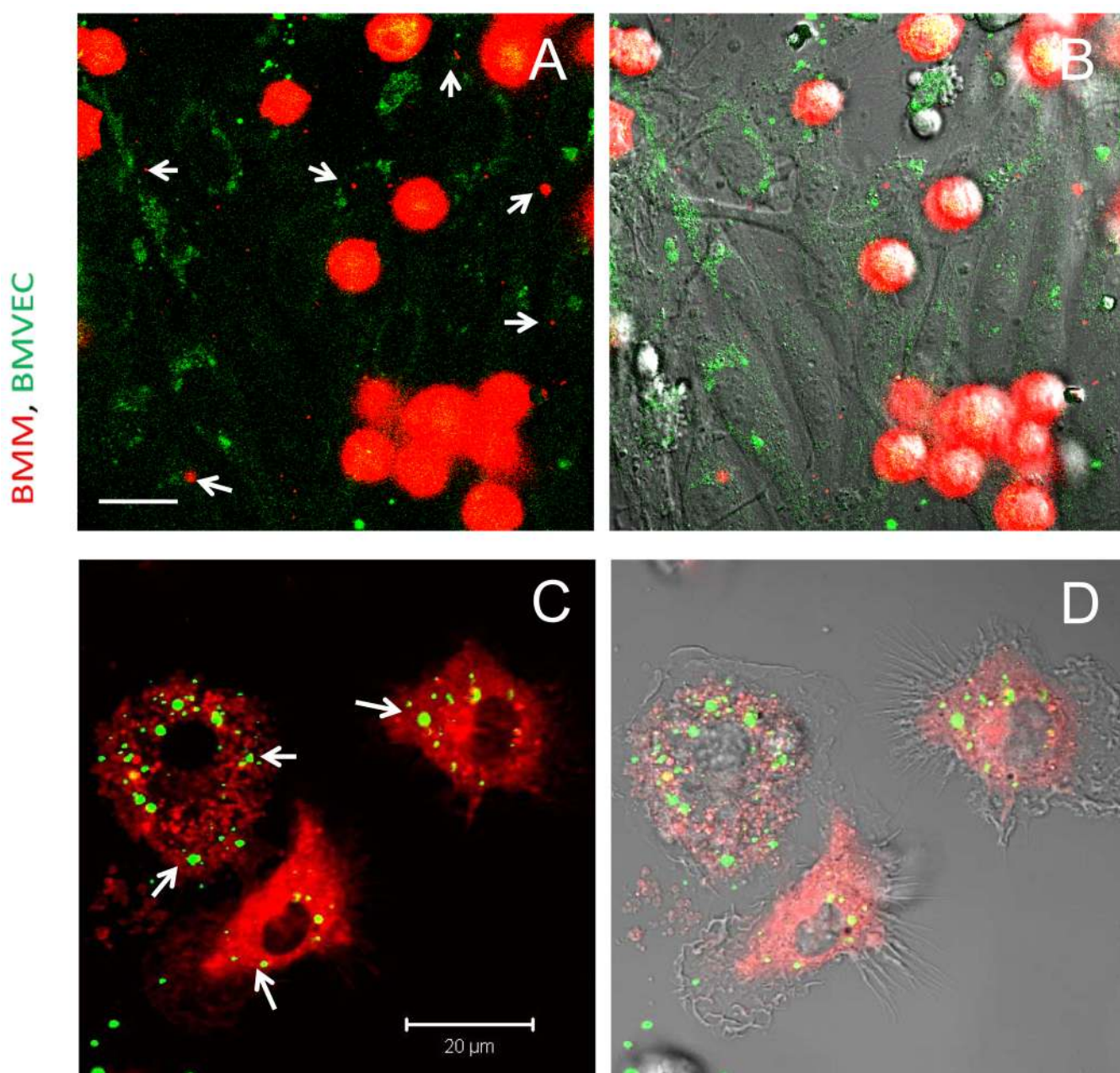
Figure 6. Intercellular exchange of BMM and BMVEC lipid compartments
BMM loaded with nanozyme were stained with DID dye (red) and incubated with BMVEC stained with DIO dye (green), Cells were cultivated one with the other at 37°C for two hrs. Following incubation cells co-cultures were washed with PBS and visualized by confocal microscopy. **A, C**, fluorescent images only; **B, D**, fluorescent images with DIC are shown. Images demonstrated presence of red vesicles from BMM in BMVEC cells (**A, B**), and green vesicles from BMVEC in BMM (**C, D**) pointed with arrows. Bar represents 20 µm.
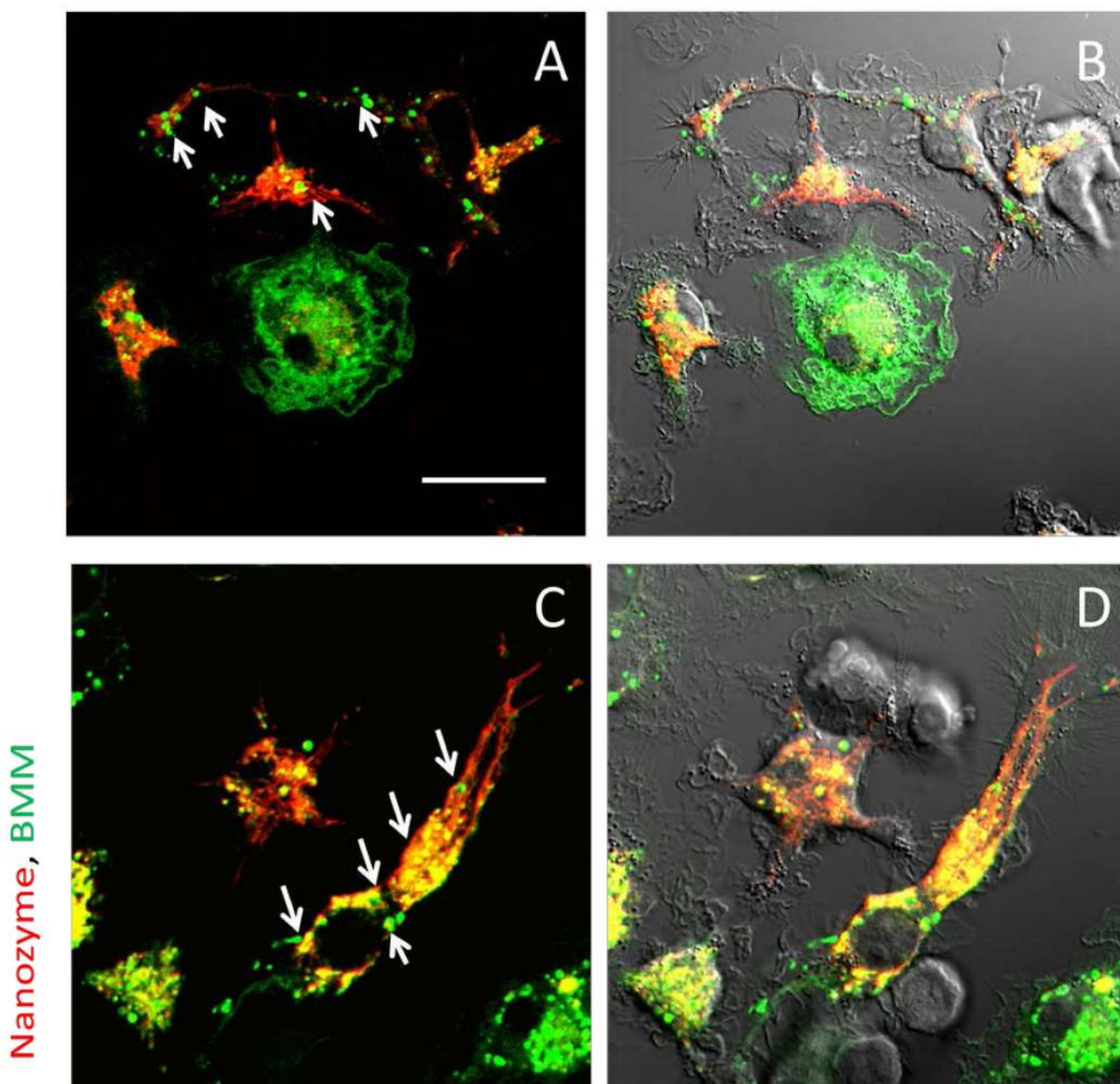
Figure 7. Transfer of nanozyme along with lipid compartments from BMM to neurons
RITC-labeled nanozyme (red) was loaded into BMM labeled with DIO (green), and added to Cath.A neurons. Following a two-hour incubation, the cells were washed with PBS then visualized by confocal microscopy. **A, C**, fluorescent images only; **B, D**, fluorescent images with DIC. Images show red nanozyme co-localized with green vesicles (lipids) from BMM in Cath.A neurons. These are seen by arrows. Bar represents 20 µm.
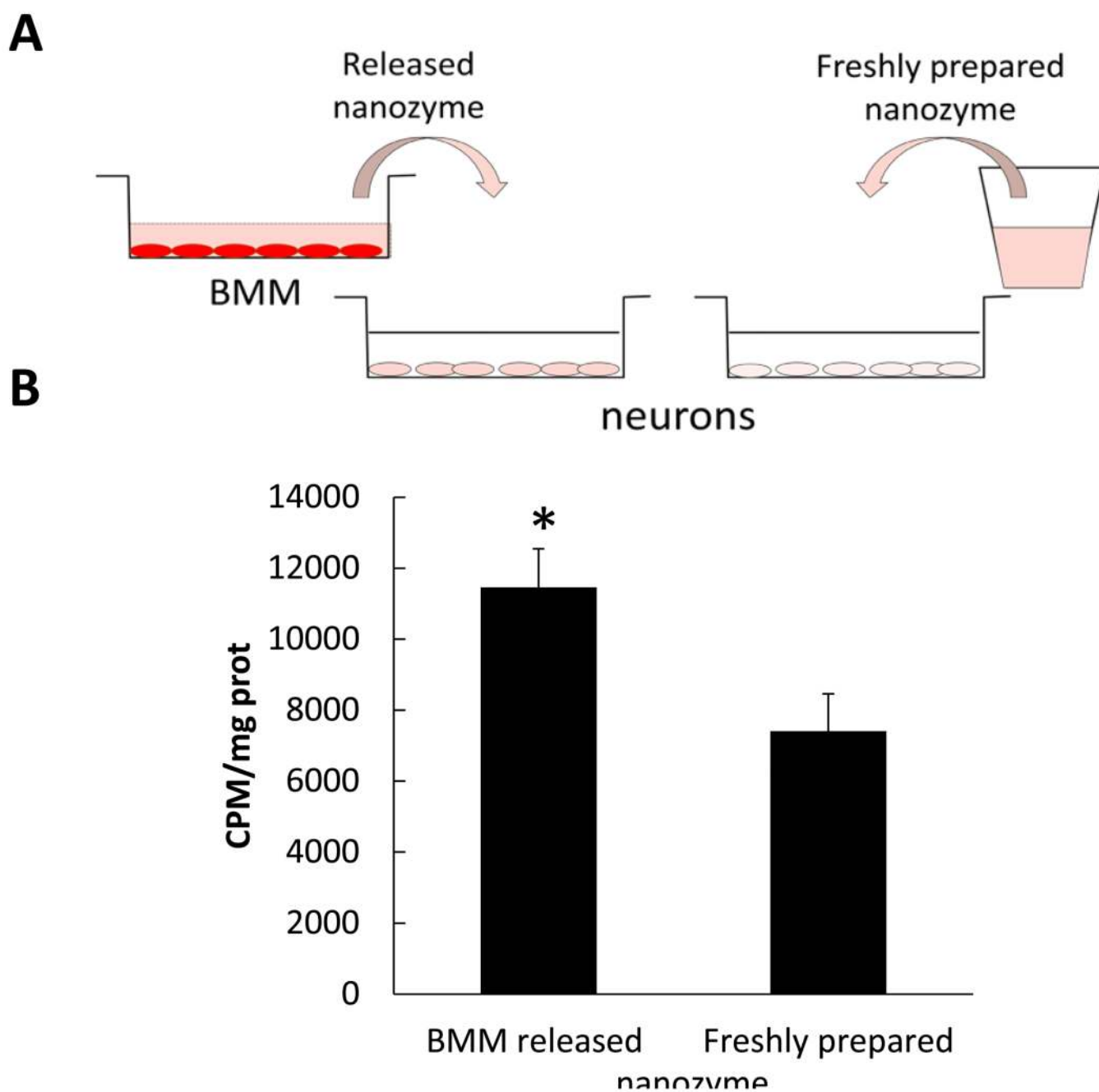
Figure 8. Facilitated transport of nanozyme released from BMM to neurons
Loaded with ^{3}H-labeled catalase nanozyme BMM were incubated in assay buffer for at 37°C for two hrs. Nanozyme released into the media was collected then added to Cath.A neurons for an additional two hrs. In parallel, neurons were incubated with freshly prepared nanozyme (at the same concentration) as a control. Following incubation cells were collected and the amount of accumulated nanozyme assessed by a liquid scintillation counting. **A**, overall experimental scheme; **B**, Results from N=4 wells (± SEM) demonstrated that nanozyme released from BMM accumulated in neurons at greater levels than freshly prepared nanozyme. Statistical significance is shown by asterisk: *p<0.05* (*).
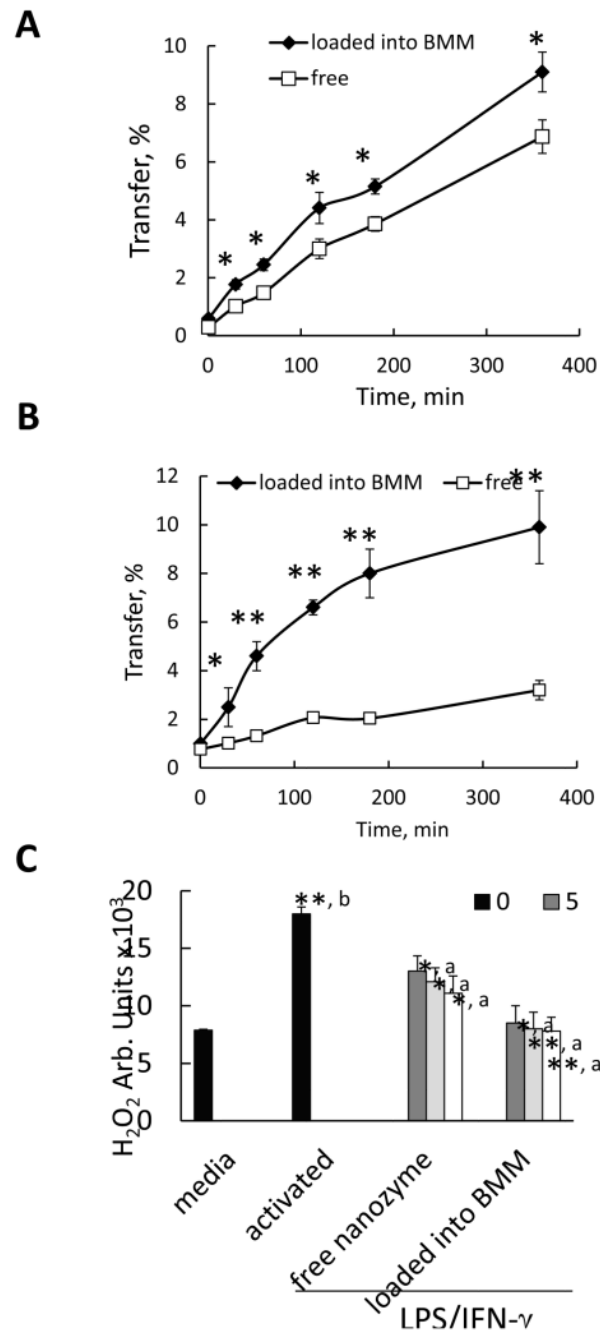
Figure 9. BMM-mediated transfer of nanozyme to endothelial cells and neurons
Effect of nanozyme loading into BMM on its transport across BBB *in vitro* (**A, B**), and its antioxidant activity in human monocyte-derived ROS (**C**). **A, B**, ^{3}H-labeled nanozyme loaded into BMM (filled diamonds), or nanoparticles alone (empty squares) were added to the donor (upper) chamber with **A**, BBMEC monolayers; or **B**, Caco-2 monolayers. Aliquots from the receiver (lower) chamber were taken at different time points and radioactivity was recorded. **C**: Blood human monocytes were stimulated with LPS (20 ng/ml) and IFN-γ (2 µg/ml) for 24 hours. Then the cells were supplemented with: various concentrations of free nanozyme (third group) or nanozyme loaded into BMM (fourth group). A concentration of nanozyme in the media added to the activated monocytes varied from 0 to 50 µg/ml. Control

non-activated BMM (first bar) or activated BMM without subsequent treatment with nanozyme (second bar) were incubated with fresh media. Following incubation, the cell media was supplemented with Amplex Red and HRP solutions. Amount of H_2O_2 produced by BMM and decomposed by catalase nanozymes after 90 min was detected by fluorescence. Results from N=4 wells (± SEM) clearly demonstrated that nanozyme transport across an *in vitro* BBB (**A and B**), and the enzymatic activity of nanozymes (**C**) from the cell-carriers was substantially greater, compared to the transport and activity of free nanozyme. Statistical significance is shown by asterisks: (*) $p<0.05$, and (**) $p<0.005$. For antioxidant activity studies (**C**) statistical significance was compared with: a) activated cells, and b) non-activated BMM.
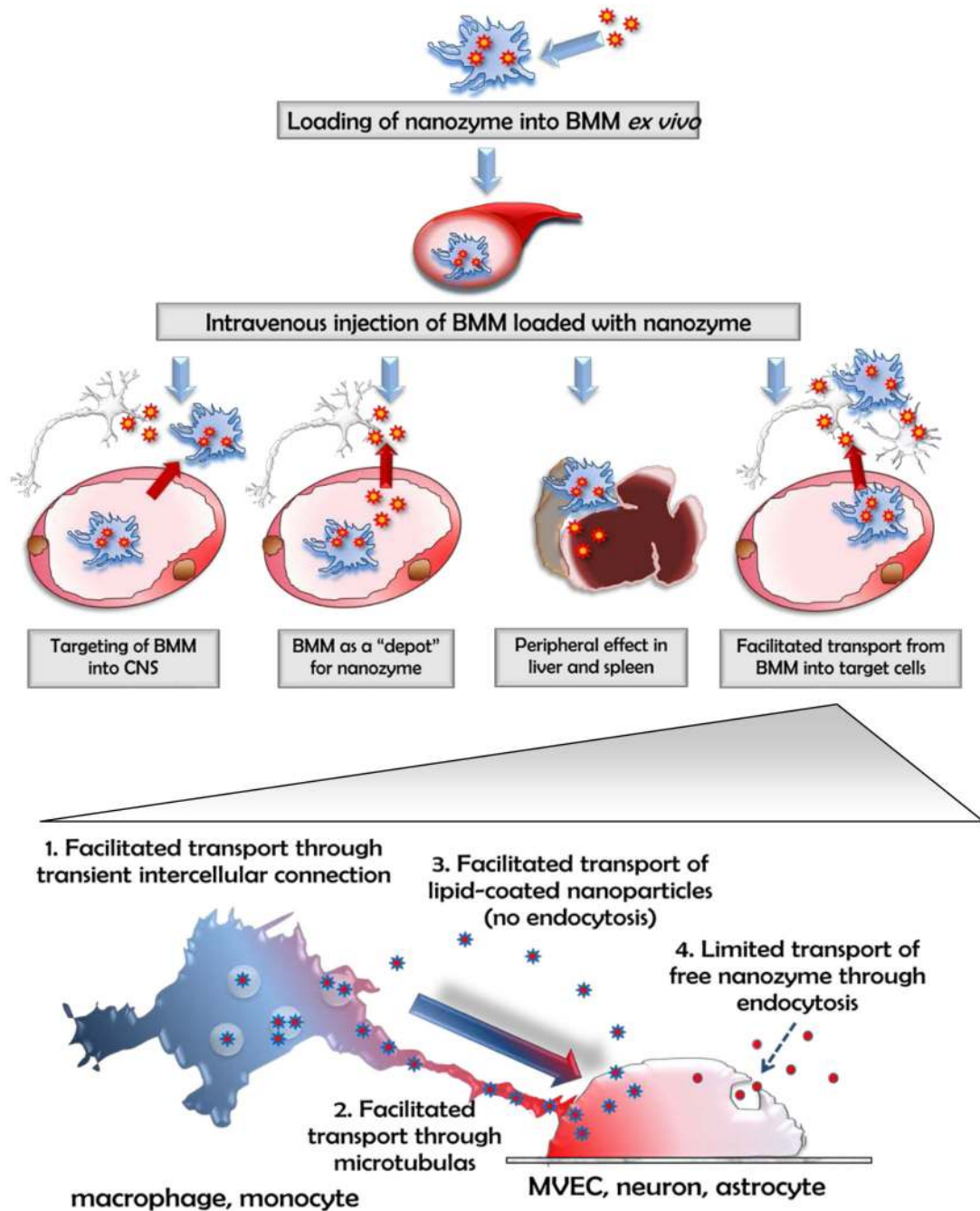
Figure 10. A pictorial scheme for cell-based nanoformulated drug delivery
Four possible ways of BMM-mediated therapeutic effects of catalase nanozyme in PD mouse model: **Pathway I**: BMM loaded with nanozyme cross the BBB and release catalase in SNpc; **Pathway II:** nanozyme is released from BMM to the blood stream and bypass the BBB independently of cell-carriers; **Pathway III:** BMM released catalase nanozyme in the liver and spleen suppressing peripheral leukocyte activation that may result in decrease of inflammation in the brain; **Pathway IV**: loaded with nanozyme BMM interact with the target cells and facilitate transfer of nanozyme from the cell-carriers into brain MVEC, neurons, and astrocytes.

Table 1

Effect of adhesion inhibitors on nanozyme transfer from BMM into target cells

Target Cells	Trypsin, % of control [*]	Locostatin, % of control [*]
BBMEC	118± 5 (n.s.)	99 ± 5 (n.s.)
Cath.A neurons	115 ± 4 (n.s.)	110 ± 5 (n.s.)

[*] Accumulation levels of nanozyme are calculated as a percentage of those treated in the absence of the adhesion inhibitors.

Table 2

Effect of energy depletion on nanozyme transfer from BMM to target cells

Target Cells	Nanozyme-loaded BMM, % of control [*]	Free nanozyme, % of control [*]
BMVEC	102 ± 5 (n.s.)	51 ± 2 ([**])
Cath.A neurons	101 ± 4 (n.s.)	37 ± 5 ([**])
BBMEC	100 ± 3 (n.s.)	49 ± 2 ([**])

[*] Accumulation levels of nanozyme are calculated as a percentage of those in control cells treated in assay buffer with glucose in the absence of inhibitors of ATP synthesis (50 mM 2-DG and 150 µM sodium azide).

Statistical significance compared to accumulation levels in assay buffer with glucose is shown by asterisk: *p<0.005* (**).